Slowly positively drifting bursts (SPDBs) in the 0.8-2.0 GHz range and SDO/AIA observations

Astronomical Institute of the Czech Academy of Sciences

Alena Zemanová, Marian Karlický, Jana Kašparová, Jaroslav Dudík

[1] *Astronomical Institute of the Academy of Sciences of the Czech Republic, Fričova 298, 251 65 Ondřejov, Czech Republic*

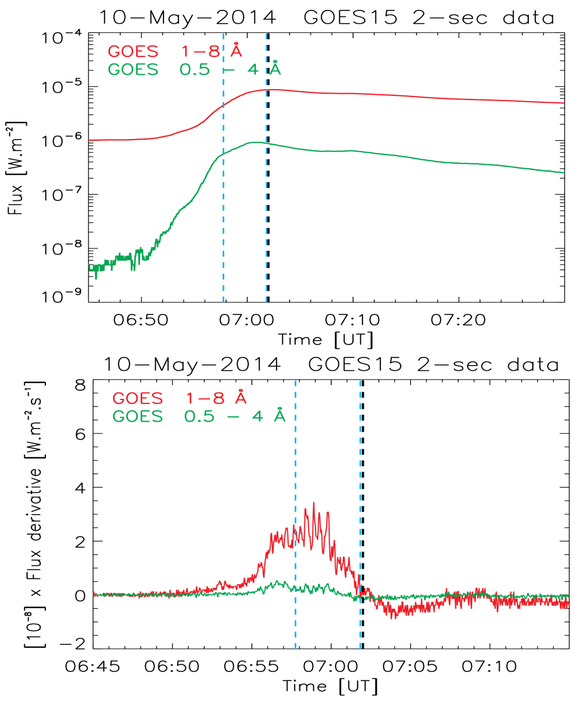

Figure 1: (Top) SXR flux as measured by GOES15. Black dashed line denotes the flare maximum in SXR and blue dashed lines show time interval when SPDBs occurred. (Bottom) Derivative of GOES flux blue lines show that SPDBs occurred during the impulsive phase of the C8.7 flare (06:51-07:02-07:30 UT).

Radio bursts with the slow positive frequency drift in the range of 0.8-2.0 GHz are quite rarely observed and their origin is still under discussion (*Jiřička & Karlický 2015, CEAB 39, 59*; *Karlický et al. 2018, ApJL 854, L29*; *Zemanová et al. 2020, ApJ 905, 111*). In general, it is not straightforward to associate flare events, or phenomena in flares, with observed radio bursts (*Bisoi et al. 2018, ApJ 862, 65; Yan et al. 2021, FrASS 8, 20; Bataglia et al. 2021, ApJ 922, 134*).

Using SDO/AIA observations, we try to infer what flare features/loci could be associated with observed SPDBs. We constructed light curves from several bright kernels observed within flare ribbons and compared their time evolution with the radio flux at frequency 1.2 GHz. We found that at least two kernels are associated with SPDB. One was located within the flaring active region (close to the sunspot) and the other one was lying in the south-east of the active region. Moreover, SDO/AIA images showed that these two areas were connected by a large-scale flare loop. Therefore we propose that the source of this SPDB could be within this loop, even HXR source was observed only at one of its footpoints.

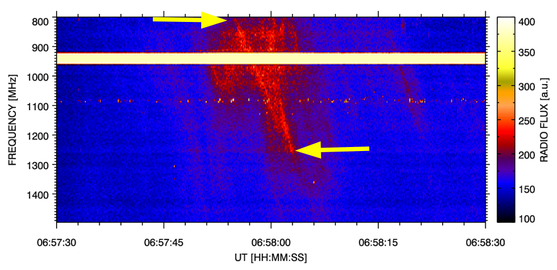

Figure 3: Detail of the most prominent SPDB which lasted about 9s (06:57:54 UT – 06:58:03 UT) with drift of 56 MHz.s^{-1}. The arrows show approximately its start and end. When considering plasma emission mechanism of the burst, the spectrum can provide us with density of the plasma where it occurs (app. F: 8x10^{9}-2x10^{10} cm^{-3} ; H1: 2x10^{9}-5x10^{9} cm^{-3}) but it does not provide any information about the burst localozation.

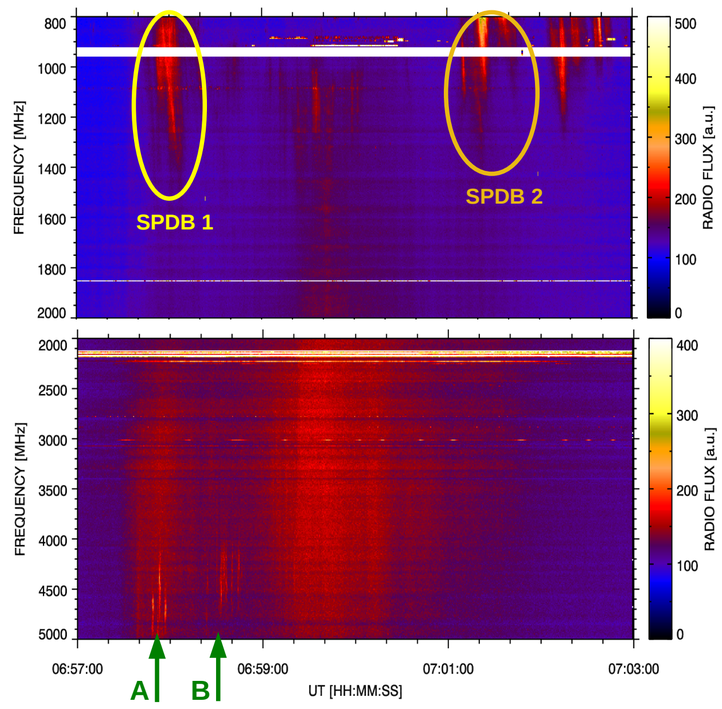

Figure 2: Radio spectrum from Ondřejov radiospectrographs RT5 0.8-2.0 GHz (top) and RT4 2.0-5.0 GHz (bottom). Yellow ellipse marks the SPBD 1 studied here and its detial can be seen in Figure 3. The second SPDB 2 can be seen between 07:01:15-07:01:30 UT (orange ellipse). The spectrum in 2.0-5.0 GHz is dominated by continuum esmission and there are two sets of type III burst: A and B (arrows). The first one was observed before and the second after the studied SPDB 1.

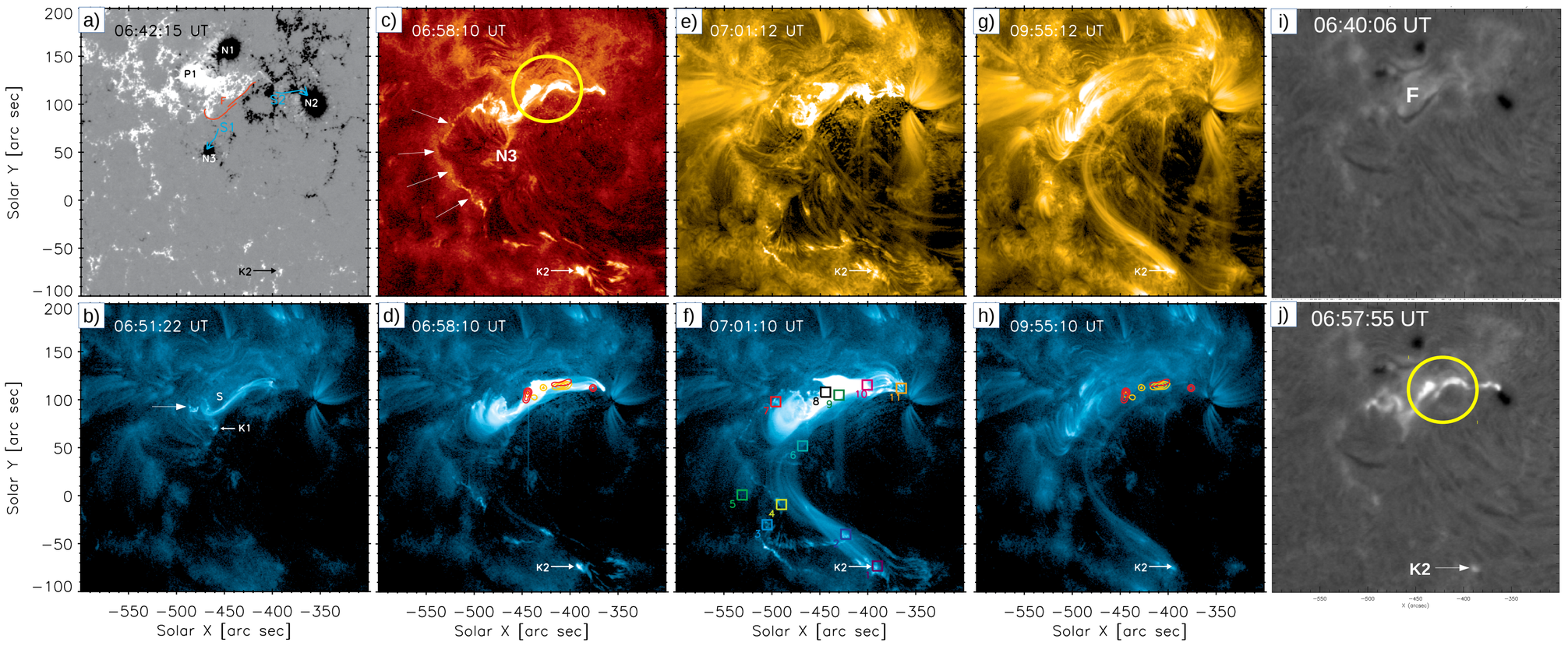

Figure 4: SDO/AIA, HMI and Hα images (KSO) showing the flare evolution.
(a) HMI line-of-sight magnetogram of NOAA AR 12 056. The filament F is shown in red. Flare started by activation of F (i) seen as bright sigmoid S in 131 Å (b). Two bright kernels appeared next to S (arrows on b). They were connected by tiny loops slipping from K1 towards N3 (blue path S1 in a). From 06:53 UT a new negative ribbon appeared (blue path S2 in a). The S enlarged and two parllel ribbons (c, j), with HXR sources (d: 12-25 keV orange, 25-50 keV red), were observed in its central part. The S interacted with the separatrix dome of the negative polarity sunspot N3 and new positive ribbons appeared at its border (c - arrows). Simultaneously a bright kernel K2 appeared far south of S (c-h). K2 was intensive in all AIA filters and also Hα (j). At the location of K2 a large-scale flare loop started to fill up with hot plasma (cf. (e) and (f)). Three hours after the flare maximum (g, h) we observed a bundle of large-scale loops connecting area of K2 with N2 and the small negative polarity next to it (a).

As the K2 appeared during the time of radio bursts (Type IIIs and SPDB 1), we constructed a light curve from this area in UV 1600 Å filter, as well as from other places within positive and negative ribbons, to see the time evolution of their intensity. Locations of these areas can be found in (f).

Light curves: RHESSI, Radio 1190, 4300, 4680 MHz, and SDO/AIA 1600 Å

Figure 5: (Top) RHESSI conut rates for two energy channels : 12-25 keV (green) and 25-50 keV (Blue). HXR flux in 12-25 keV started to rise from 06:53 UT and 25-50 keV channel raised from about 06:55 UT. (Note that a peak about 07:02 UT (violet arrow) belongs to the attenuator changing.)
(Bottom) cuts through the radio spectrum at three frequencies: 1190, 4300 and 4680 MHz. Radio bursts are labelled.

The first set of type III burst (A) (Fig. 2) occurred about 06:57:47 - 06:57:57 UT and the second set of type III bursts (B) occurred about 06:58:22 – 06:58:46 UT. These type III bursts were observed at rather high frequencies: 4.0-5.0 GHz. The studied SPDB 1 was observed at 06:57:54 UT – 06:58:03 UT (dotted line).
Both type III bursts A and B together with SPDB 1 occurred about the maximum of the first HXR peak of 25-50 keV while the second SPDB 2 (dotted line) was observed at 07:01:15-07:01:30 UT, during the decline of the second HXR peak at 25-50 keV. This suggests that for SPDBs the occurrence of HXR peaks in 25-50 keV is not necessary. On the other hand there is good time correspondence between continuum radio emissionon at frequencies 2.0-5.0 GHz and HXR peaks of 25-50 keV.

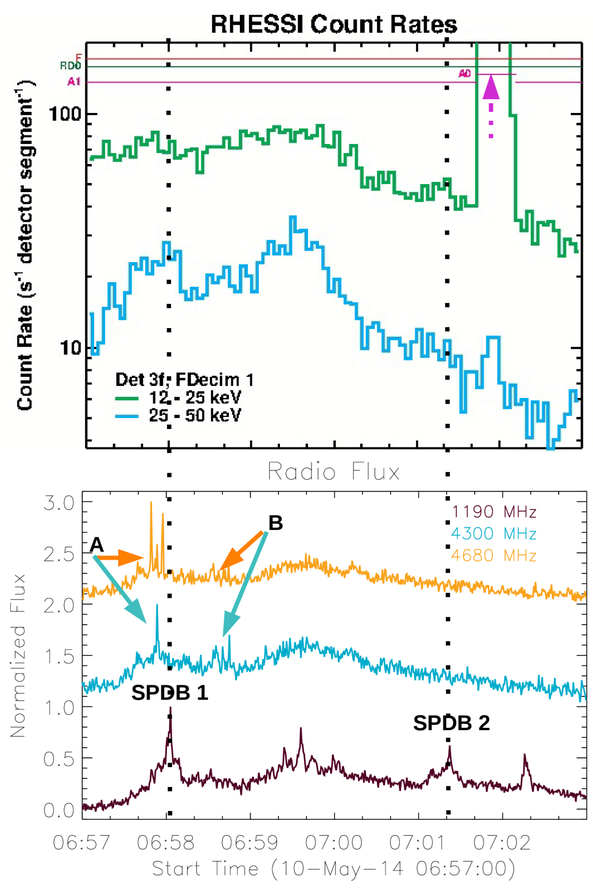

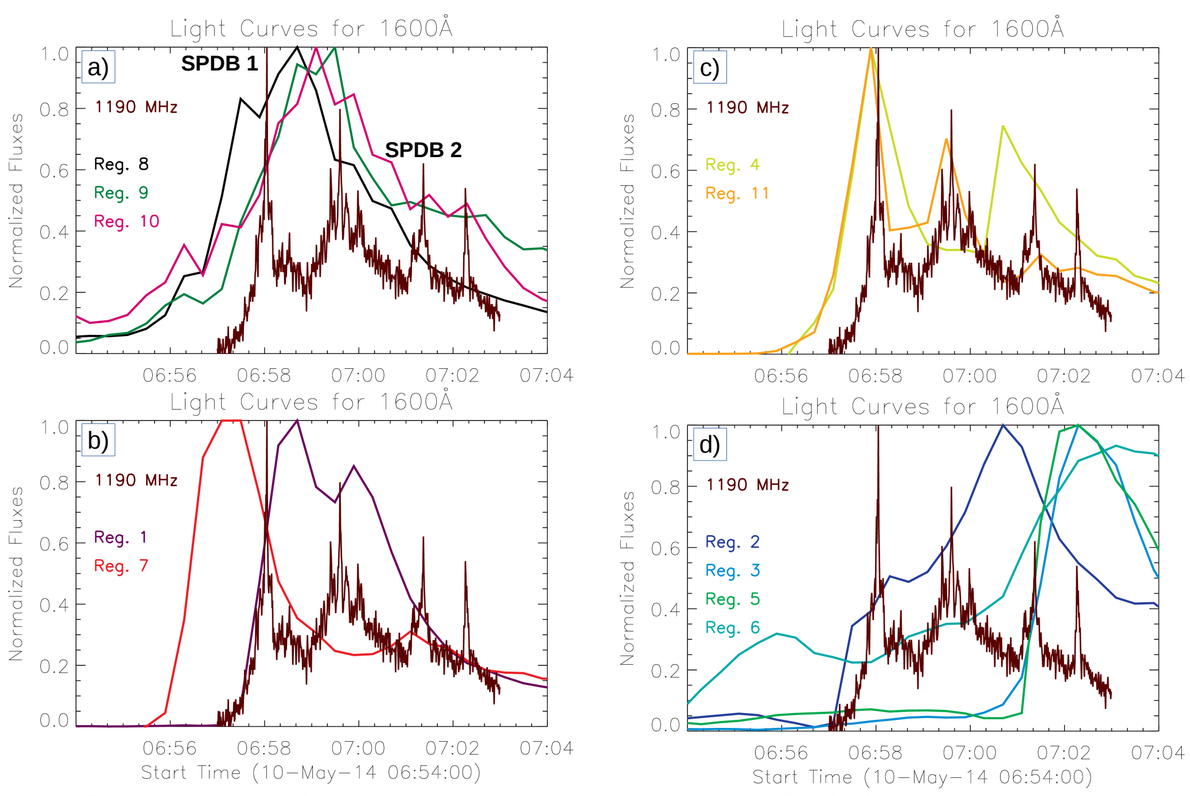

Figure 6. The light curves (LCs) from several regions over the flare ribbons (see Fig. 4f, with colours respectively as here) observed in AIA 1600 Å filter. The emission in this filter comes mostly from ribbons and is less influenced by appearance of flare loops. The disadvantage of this filter is its low cadence 30s contrary to 12s of EUV.

Figure 6 (continue): Panel (a) shows a comparison of the cut of radio spectrum at 1190 MHz (brown) and three regions located within parallel ribbons (8, 9, 10; Fig. 4f). Their LCs rise earlier than any radio bursts occurred. Their maxima fall within time interval 06:58:20-06:59:40 UT and their loci correspond to RHESSI HXR kernels (Fig 4d, f). Therefore we suggest that they are likely associated with type III bursts and sheared flare loops. Panel (b) shows LC from 1190 MHz, reg. 1 and reg. 7. The LC for reg. 1, which is identical with K2 in Fig. 4, has two maxima and both are shifted plus 20 to 40s relative to the time of the closest radio burst. Very interesting is the rising part of its LC which coppies the rise of SPDB 1. Reg. 7 is approximately located in the area where the interaction of S and the separatrix dome of N3 sunspot started. Its peak occurred before any of radio bursts were observed. Panel (c) LCs from reg. 4 and 11 follow the observed radio bursts best. That for reg. 4 has two peaks. The first occurred just few seconds before SPDB 1 while the second one preceeds SPDB 2 of app. 40s. Reg. 4 lies on the positive ribbon surrounding the dome of N3 sunspot (Fig. 4a, c and f). LC of reg. 11 posesses 3 peaks and each is located just a few seconds about the peak of the observed radio bursts: SPDB 1, SPDB 2 and also a group of bursts inbetween them (Fig. 2, top). Fig. 4g and 4h show that reg. 1 (K2) and reg. 11 are connected by a large-scale flare loop. We suggest, that very likley, the radio source of SPDB 1 is conncted with this loop. Panel (d) shows LCs for four regs. 2, 3, 5 and 6. The LC for reg. 2 has the main peak that covers several bursts with maximum happening before SPDB 2. LCs for reg. 3, 5 peak after SPDB 2 and they belong to ribbons that appear about the maximum of the flare. Reg. 6 is centered on the sunspot N3 (Fig. 4a) and the evolution of its LC is very likely associated with activity close to/along the spine of the separatrix dome of N3 sunspot.

ACKNOWLEDGEMENTS

A.Z. , M.K., J.K., J.D. acknowledge Grants No. 20-07908S, 20-09922J, 21-16508J, 22-34841S of the Grant Agency of the Czech Republic, as well as institutional funding RVO:67985815 from the Czech Academy of Sciences. Courtesy of NASA/SDO and the AIA, EVE, and HMI science teams. H-alpha data were provided by the Kanzelh öhe Observatory, University of Graz, Austria. We acknowledge the use of the RHESSI Mission Archive available at https://hesperia.gsfc.nasa.gov/rhessi/mission-archive.